AWARD NUMBER: W81XWH-19-1-0378

TITLE: Combining Androgen Deprivation and Immunotherapy to Prevent Progression to Castration-Resistant Prostate Cancer

PRINCIPAL INVESTIGATOR: John J Krolewski, MD, PhD

CONTRACTING ORGANIZATION: Health Research, Inc.
Health Research-Roswell Park Cancer Inst
Buffalo, NY

REPORT DATE: October 2021

TYPE OF REPORT: Annual

PREPARED FOR: U.S. Army Medical Research and Development Command
Fort Detrick, Maryland 21702-5012

REPORT DOCUMENTATION PAGE

Form Approved
OMB No. 0704-0188

1. REPORT DATE	2. REPORT TYPE	3. DATES COVERED
October 2021	Annual	01Sep2020-31Aug2021

4. TITLE AND SUBTITLE
Combining Androgen Deprivation and Immunotherapy to Prevent Progression to Castration-Resistant Prostate Cancer

5a. CONTRACT NUMBER
W81XWH-19-1-0378

5b. GRANT NUMBER
PC180278

5c. PROGRAM ELEMENT NUMBER

6. AUTHOR(S)
John J. Krolewski, MD, PhD

E-Mail: john.krolewski@roswellpark.org

5d. PROJECT NUMBER

5e. TASK NUMBER

5f. WORK UNIT NUMBER

7. PERFORMING ORGANIZATION NAME(S) AND ADDRESS(ES)

Health Research, Inc.
Health Research-Roswell Park
Cancer Inst
Elm and Carlton St
Buffalo NY 14263-0001

8. PERFORMING ORGANIZATION REPORT

9. SPONSORING / MONITORING AGENCY NAME(S) AND ADDRESS(ES)

U.S. Army Medical Research and Development Command
Fort Detrick, Maryland 21702-5012

10. SPONSOR/MONITOR'S ACRONYM(S)

11. SPONSOR/MONITOR'S REPORT NUMBER(S)

12. DISTRIBUTION / AVAILABILITY STATEMENT

Approved for Public Release; Distribution Unlimited

13. SUPPLEMENTARY NOTES

14. ABSTRACT

Recently, we found that in a PTEN-deficient mouse PCa model, castration induces an immunosuppressive state within the tumor that is concurrent with tumor recurrence. Mechanistically, this response to ADT is mediated by soluble mediators (TNF and CCL2), facilitating communication between tumor, stromal and immune cell populations within the tumor microenvironment. Based on these preliminary data, we hypothesize: Blocking myeloid suppression prevents progression to castration resistant prostate cancer. We test this hypothesis in three aims. Aim 1 examines the mechanism of paracrine TNF signaling between tumor, stromal and myeloid cell populations within the TME, in inducing immune suppression following ADT. Aim 2 tests whether blocking the transit and/or function of myeloid suppressive cell populations prevents CRPC (tumor recurrence following ADT). We also determine the role of PTEN in ADT-induced immune evasion. Aim 3 tests the hypothesis that ADT, in men with locally advanced PrCa, increases serum TNF and CCL2, as well as circulating myeloid cells, by assessing samples from an ongoing clinical study.

15. SUBJECT TERMS
androgen, castration, immunotherapy, prostate, cancer, TNF, CCL2, tumor associated macrophages, CD8 T-cells

16. SECURITY CLASSIFICATION OF:			17. LIMITATION OF ABSTRACT	18. NUMBER OF PAGES	19a. NAME OF RESPONSIBLE PERSON
a. REPORT	b. ABSTRACT	c. THIS PAGE			19b. TELEPHONE NUMBER *(include area code)*
Unclassified	Unclassified	Unclassified	Unclassified	15	

TABLE OF CONTENTS

1. INTRODUCTION:

Most prostate cancer (PCa) deaths are due to castration resistant PCa (CRPC). While androgen deprivation therapy is the standard of care for patients with advanced PCa, nearly universal progression to CRPC occurs 2-3 years after ADT is initiated. Although there have been key advances in the treatment of CRPC, even the best therapies are not curative. One approach to this problem is to improve the initial treatment of advanced prostate cancers, by combining complementary therapies with ADT, to prevent progression of such advanced cancers to CRPC. Immunotherapy, typically employing T-cell 'checkpoint' inhibitors, has provided very durable remissions, verging on cure for a variety of cancer types. However, CPIs have *not* been effective in prostate cancers, perhaps because such cancers are 'cold' (lacking cytolytic CD8 T-cells). Cold tumors may be caused by infiltration of myeloid cell populations – tumor associated macrophages (TAMs) and myeloid-derived suppressor cells (MDSCs) – into the tumor immune cell microenvironment (TIME). In preliminary data accompanying this proposal, we demonstrate that castration of a PTEN-deficient mouse PCa model induces an immunosuppressive state within the tumor that is concurrent with the onset of tumor recurrence. The response to castration/ADT is tri-phasic: a pro-apoptotic regression phase where tumor shrinks, followed by selection for a residual population of resistant stem-like tumor cells and finally recurrent growth as CRPC. Using PCa cell lines to model the first two phases of the response to ADT, we have shown that ADT induces apoptosis, thereby enriching for an ADT-resistant stem/progenitor population that we demonstrate is an *in vitro* source of enhanced TNF production. Mechanistically, in our model system the response to ADT is driven by the soluble mediators TNF and CCL2, which facilitate communication within the TIME. Specifically, a TNF-CCL2-CCR2 paracrine loop is induced between prostate cancer cells and non-tumor cells in the microenvironment: TNF produced by tumor cells acts on myofibroblasts and TAMs to induce CCL2 production, which in turn recruits tumor-associated macrophages (TAMs) and possibly MDSCs. Analysis of public PCa data sets shows TNF and stem/progenitor marker expression are both increased in CRPC, consistent with our hypothesis that ADT drives the development of an immuno-suppressive state via a cytokine switching mechanism that triggers the TNF-CCL2-CCR2 axis in the TIME.

2. KEYWORDS:

androgen, castration, immunotherapy, prostate, cancer, TNF, CCL2, tumor associated macrophages, CD8 T-cells, myeloid-derived suppressor cells, CCR2, TNF receptors, tumor microenvironment

3. ACCOMPLISHMENTS:

What were the major goals of the project?

We proposed that TNF promotes an immunosuppressive state via CCL2, to drive castration-resistant tumor growth.

- Aim 1 determines the role of tumor-microenvironment-derived TNF as a trigger to induce vascular regression following ADT.

- Aim 2 tests our immune suppression hypothesis in three sub-aims.
- Aim 3 tests the hypothesis that ADT administered to men with locally advanced PCa increases serum TNF and CCL2

What was accomplished under these goals?

Accomplished under Aim 1:

In the first year of this grant, we completed Major task 1but found that we were unable to proceed with the remainder of the aims, due to limitations of the experimental systems we had previously identified for use in the proposal. We revised Aim 1 and have now completed the remainder of Aim 1 (revised Major Task 2 and revised Major Task 3).

First we describe the accomplishments under Aim 1, Major Task 2:

(revised) Major Task 2: Determine if ADT/castration induces a TNF-dependent change in the tumors vascular network	Months	100 mice	None
Subtask 1: Develop tumor system for studies (hiMYC allografts in the flanks of FVB mice) and	12-15		
Subtask 2: Perform pilot studies to optimize CD31 IHC vascular network analysis and determine optimal timing post-castration	16-19		
Subtask 3: Castrate mice (+/- TNF blockade); assay vascular damage via anti-CD31 IHC; determine effects on various vascular parameters (vessel size, etc)	20-24		

Subtask 1:

Ultrasound imaging with co-registered photoacoustic imaging (PAI), power Doppler, contrast-enhanced ultrasound (CE-US) and B-mode high-resolution, HFUS imaging were performed using a 256 element, 21MHz linear-array transducer (LZ-250) and the Vevo LAZR system (VisualSonics Inc., Toronto ON, Canada). After mice were anesthetized and depilated, B-mode ultrasound images were acquired from the peritoneum, and 3D reconstructions of the prostate tumors were computed using Amira 3D visualization software (FEI Visualization Sciences Group) (26). For power Doppler sonography parameters used for acquisition were: operating frequency: 16MHz, pulse repetition frequency: 2kHz, Doppler gain: 40, depth: 20.00 mm, width: 23.04 mm, clutter/wall filter: medium. To enable accurate comparison of power Doppler data, the relative change in power Doppler signal was calculated for the 3D ROI covering the entire tumor. Multispectral PAI was performed to obtain measurements of oxygen saturation (sO2). PAI parameters used were: Operating frequency 21 MHz, Depth: 23.00 mm, Width: 23.04 mm, Wavelength: 750/850 nm, total hemoglobin concentration

threshold (Hbt) was 20 arbitrary units, acquisition mode: sO2/Hbt. The photoacoustic gain was kept at 43 dB and dynamic range at 20 dB for all studies. PAI based measurements of oxygen saturation were calculated using the two-wavelength approach (750/850 nm) as described (28, 29). Nonlinear Contrast Mode imaging was performed to detect the presence of Vevo MicroMarker contrast agent (VisualSonics, Toronto, ON, Canada). The contrast agent consists of phospholipid shell microbubbles filled with nitrogen and perfluorobutane (2.3 to 2.9 μm in diameter). A bolus injection of the contrast agent ($1x10^8$ microbubbles) was administered via tail vein injection using a 25-gauge needle. Images were acquired using the following parameters: Operating frequency 18MHz, Depth: 20.00 mm, Width: 23.04 mm, with 35dB contrast gain, gate size 6. Nonlinear detection of the contrast signal was done in 3D by moving the transducer through the volume of the tumor at a step-size of 0.152 mm. Multimodal imaging datasets were processed offline using VEVO CQ software utilizing manually drawn tumor regions with perfusion parameters derived from intratumoral signal intensity time curves. All imaging datasets were analyzed using Vevo LAB (v.1.7.2) workstation software.

To establish the Myc-CaP tumors, both flanks of male FVB/NCr mice (8-12 week old, Charles River Labs) were injected with $5x10^5$ Myc-CaP/ARE-luc cells re-suspended in equal volumes of RPMI media and Matrigel (Corning, Bedford, MA). Tumor development was monitored by palpation and when evident, quantitated by high-frequency ultrasound (HFUS) imaging, as described above. Mice were treated and castrated or sham castrated within 17 days of tumor cell injection. Average tumor volume at the time of castration was 382 +/- 120 mm^3.

Sub-task 2:

We performed optimization experiments in conjunction with the institutional core facilities to determine the conditions for IHC staining (DNS). In brief, mice were sacrificed 24h after castration and tumors collected for histology. Tumors were fixed in formalin-free immunohistochemistry zinc fixative (BD Pharmingen, San Diego, CA) and 4 μm paraffin sections obtained. Vessel damage was determined by immunohistochemistry for CD31 (rat anti-mouse CD31, clone MEC13.3, #550274, BD Pharmingen) using an autostainer (Agilent/DAKO Carpinteria, CA) as reported. Images were digitized using the ScanScope XT system. The entire tumor area was delineated using Aperio ImageScope v11 and analyzed using the default parameters of the automated microvessel analysis algorithm v1.1 (Aperio Technologies, Vista, CA). We then performed a limited amount of IHC to determine when the optimal size of tumor was reached and to optimize the time post-castration (DNS).

Sub-task 3:

We next tested if vessel structural changes, which correlate with the castration-induced functional vascular damage, are TNF signaling dependent. Myc-CaP derived tumor tissue was excised and fixed one day post-castration from both vehicle and sTNFR2-Fc treated animals. Vascular integrity indicators were quantitated using CD31 immunohistochemistry (Fig. 1A). The castration-induced reduction in micro-vessel density was reversed in two of four tumors from mice treated with sTNFR2-Fc (Fig. 1B). Intratumoral area occupied by vessels, their perimeter and the thickness of the vessel walls were each increased by sTNFR2-Fc treatment in all four tumors examined (Fig. 1C-E). These changes in the vasculature are consistent with TNF mediating the vascular structural damage induced by castration in prostate tumors.

Legend for Figure 1: Castration-induced vascular damage is reversed by TNF signaling blockade. **A,** Representative sections of CD31 immunoreactivity in Myc-CaP prostate tumor from four mice (M1-M4) castrated (upper panels) or castrated and treated with sTNFR2-Fc treated (lower panels). **B**. Microvessel density (vessels per square millimeter). **C.** Vessel cross-sectional area, in μm^2; **D,** Vessel perimeter length, in µm; **E,** Vessel wall thickness, in µm. Columns, mean of five tumors from vehicle-treated and four sTNFR2-F.+-c treated castrated mice, bars = SEM.

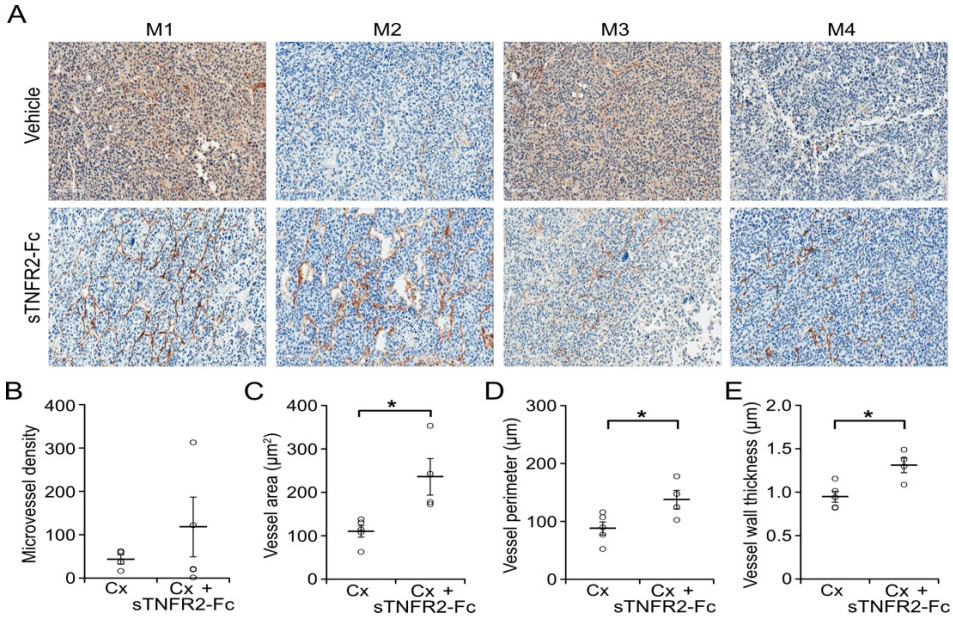

Intratumoral microvessel density is strongly correlated with power Doppler signal, and we previously reported castration reduces CD31+ vessel count. Here, while we found a mixed microvessel density increase in tumors from different sTNFR2-Fc treated host animals after castration, we demonstrate TNF is necessary for castration-induced structural vessel damage, including diameter, area, and vessel wall thickness (Fig. 1).

Next, we describe the accomplishments under Aim 1, Major Task 3.

(revised) Major Task 3: Determine if castration-induced change in perfusion, oxygenation and blood flow are TNF-dependent	Months	120 mice	None
Subtask 1: Use model developed in Major Task 2 to determine if castration induced blood flow reduction is TNF-dependent	24-26		
Subtask 2: Use model developed in Major Task 2 to determine if castration induced blood flow and perfusion reductions are TNF-dependent	27-29		
Subtask 3: Use model developed in Major Task 2 to determine if castration induced oxygenation reduction is TNF-dependent	30-32		

Subtask 1:

We tested if castration induces changes in tumor vascularity and whether induction was TNF dependent, using power Doppler imaging to quantitate the intensity of intratumoral blood flow. Doppler imaging detects vascular disruption using high-frequency sound waves to visualize blood flow magnitude. Doppler detected vascularity change may be predictive of PrCa progression and prognosis in patients, and is able to detect induced vascular disruption. Power Doppler imaging increases sensitivity versus color Doppler imaging, allowing more complete vessel function imaging by integrating speed and directional information. Castration reduced blood flow inside the tumors (Fig. 2A, 2B) but blood flow was not changed when TNF signaling was blocked using sTNFR2-Fc (Fig. 2C, 2D). The castration-induced decrease in overall tumor vascularity was TNF-dependent one day after castration, and while vascularity continued to decline, sTNFR2 treatment did not affect the castration-induced change in vascularity after four days castration (Fig. 2E, individual tumor changes at one day after castration shown Fig. 2F). Serial measurement of the change in blood flow inside the same tumor confirmed the castration reduction of blood flow was acutely TNF dependent (Fig. 2G).

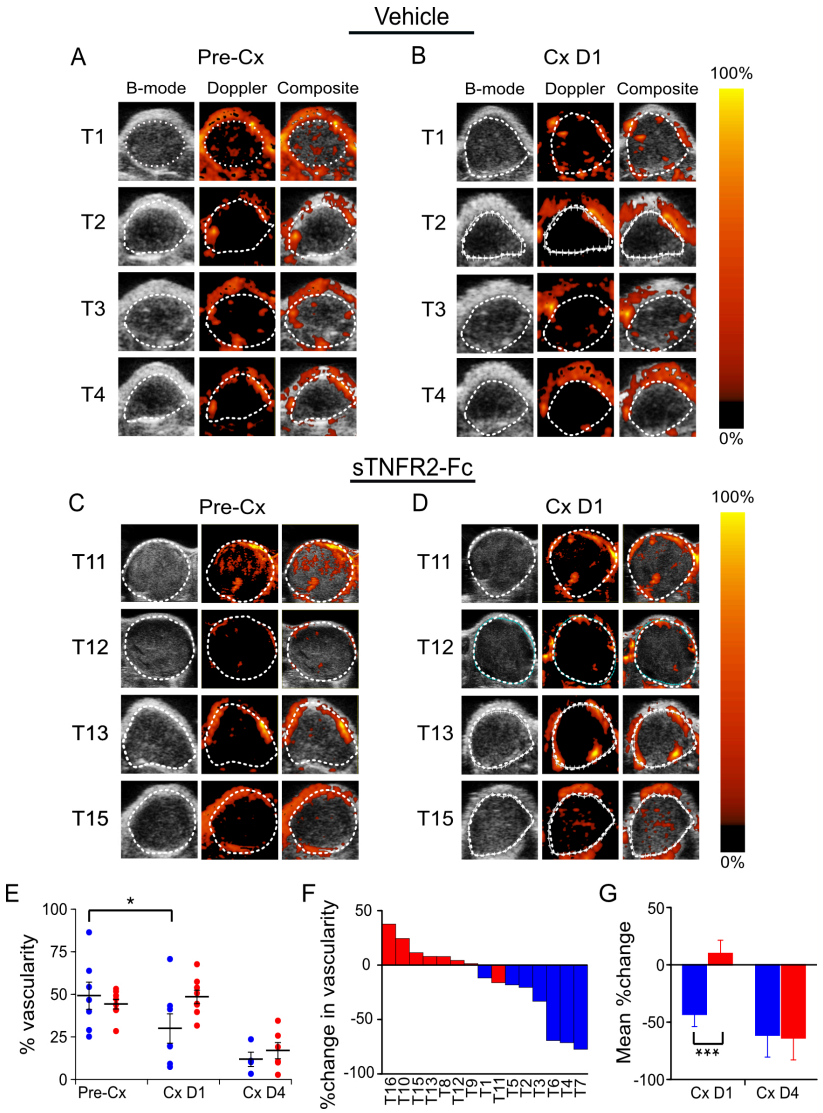

Legend for Figure 2. Castration reduction of intratumoral blood flow in Myc-CaP tumor was dependent on TNF signaling. **A,** Power Doppler (PD) images of subcutaneous Myc-CaP tumors pre-castration (Pre-Cx) of mice treated with PBS (Vehicle), tumors 1-4 (of 8 evaluable tumors). Left to right: Gray-scale ultrasound image (B-mode); PD pseudo-colored image to illustrate blood flow level (Doppler); Composite of PD image overlaid on the B-mode image (Composite). **B** PD images of tumors in panel A, one day after castration (Cx D1). **C,** PD images of a second set of subcutaneous Myc-CaP tumors pre-castration of mice treated with sTNFR2-Fc, tumors 11, 12, 13, 15 (of 8 evaluable tumors). **D,** PD images of tumors in panel C, one day after castration. **E,** Mean PD signal (% vascularity) pre-castration, and at one and four days after castration from tumors in vehicle treated (blue, D1 n=8, D4 n=7) and sTNFR2-Fc treated mice (red, D1, D4 n=8). **F,** Waterfall plot of % change in vascularity in individual tumors at one day after castration. **G,** Mean % change in paired measures of vascularity pre-castration versus D1 or D4 after castration. Columns are means and bars are SEM, *$p<0.05$, ***$p<0.001$.

Subtask 2:

To test if the changes in blood flow also resulted in reduced tumor perfusion, Myc-CaP allografts were evaluated using CE-US prior to and one-day after castration of the host animal. Relative perfusion was determined using contrast agent accumulation in tumor capillaries and quantitated from a maximum intensity projection based on contrast accumulation. Figure 3 shows castration reduced intratumoral perfusion (Fig. 3A, 3B). However, castration did not reduce intratumoral perfusion in sTNFR2-Fc pre-treated host mice (Fig. 3C, 3D). Tumors in sTNFR2-Fc pre-treated host mice were highly perfused, and this was also not changed by castration (Fig. 3E). Castration-reduction of intratumoral perfusion was dependent on TNF signaling (individual tumor changes in Fig. 3F, mean change Fig. 3G).

Legend for Figure 3. TNF signaling was necessary for castration-induced reduction in perfusion of Myc-CaP tumor. **A,** Contrast enhanced-ultrasound (CE-US) images of subcutaneous Myc-CaP tumors pre-castration (Pre-Cx) of mice treated with PBS (Vehicle), tumors 1-4 (of 7 evaluable tumors) are shown. Left to right: Gray-scale ultrasound image (B-mode); contrast-mode image prior to contrast agent injection (Pre-contrast); contrast-mode image after injection at the peak enhancement of contrast (Post-contrast); pseudo-colored image of the change in contrast enhancement (Perfusion). **B,** CE-US images of tumors 1-4 in A after one day castration (Cx D1). **C,** CE-US images of a second set of subcutaneous Myc-CaP tumors pre-castration of mice treated with sTNFR2-Fc, tumors 8, 10, 11, 12 (of 7 evaluable tumors) are shown. **D,** CE-US images of tumors in panel C, one day after castration, **E,** Mean perfusion pre-castration and post-castration in tumors in vehicle treated (blue) and sTNFR2-Fc (red) treated mice. **F,** Waterfall plot of %change in perfusion in individual tumors (columns). **G,** Average %change in perfusion pre-castration and post-castration. E, G: Columns are means and bars are SEM, *$p<0.05$, **$p<0.01$.

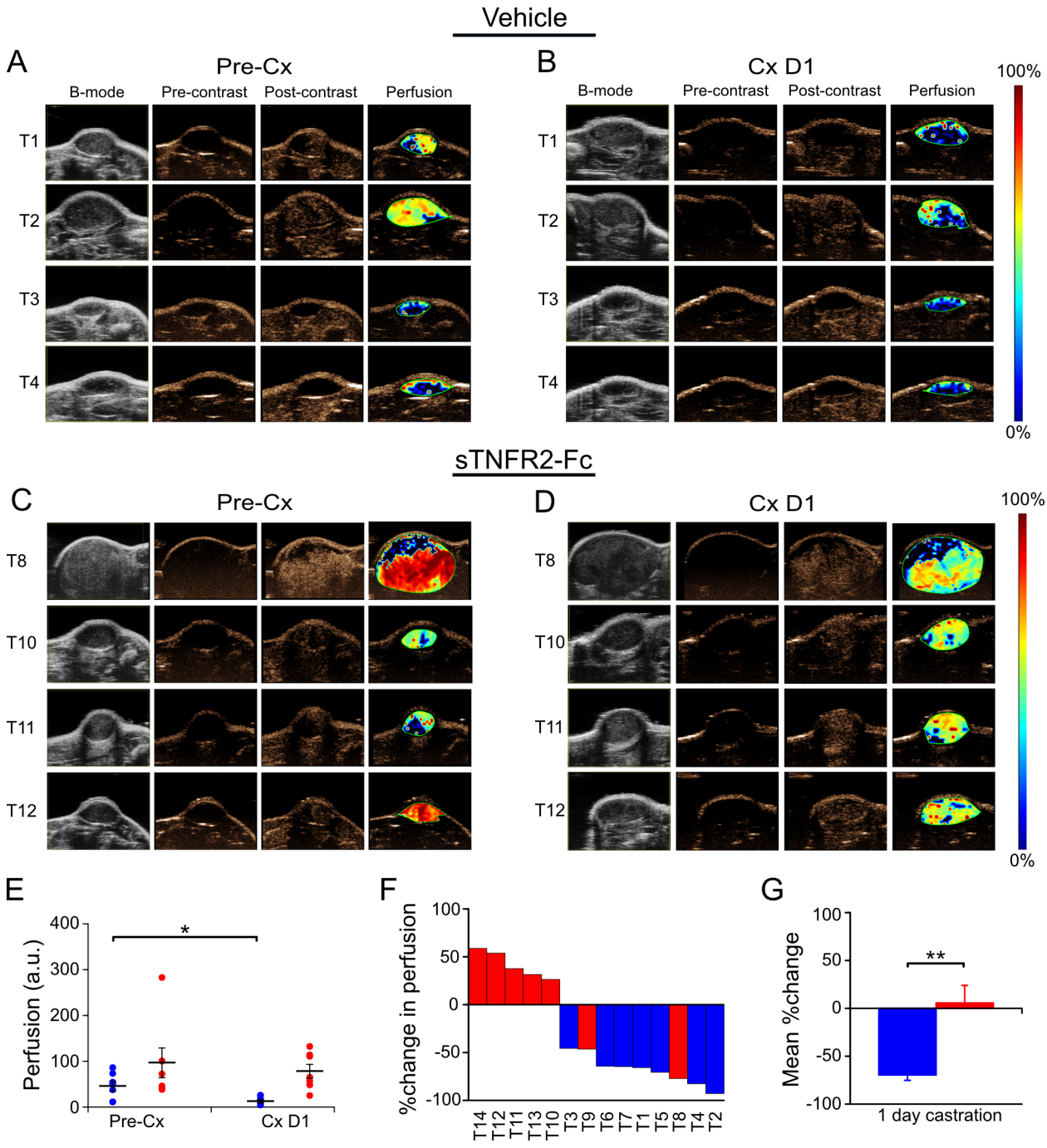

Subtask 3:

We previously observed castration reduced blood flow in Myc-CaP tumors, we therefore tested if castration also induced intratumoral hypoxia using photoacoustic imaging (PAI) to measure sO_2 concentration. PAI can discriminate the absorption spectra of endogenous oxy-hemoglobin from deoxy-hemoglobin, enabling real-time 3D visualization of microvasculature and quantitation of changes in the percent hemoglobin oxygen saturation ($\%sO_2$). When Myc-CaP allografts became palpable, tumor volume was quantitated using HFUS imaging. Host mice were pre-treated with

sTNFR2-Fc to block TNF signaling (or vehicle), and then castrated. One day after castration, photoacoustic signal was decreased (Fig. 4A) but no castration-induced change in photoacoustic signal was seen if TNF signaling was blocked using sTNFR2-Fc (Fig. 4B). Castration induced a relative decrease in intratumoral hemoglobin oxygen saturation (%sO_2) in one day after castration, but not when TNF signaling was blocked in host mice using sTNFR2-Fc (Fig. 4C, individual tumor changes shown Fig. 4D). The castration-induced hypoxia was not detectable by four days after castration. Total intratumoral hemoglobin was not changed by either castration or sTNFR2-Fc treatment (Fig. 4E). Comparison of paired oxygenation changes in the same tumor revealed the castration induction of hypoxia was TNF dependent (Fig. 4F).

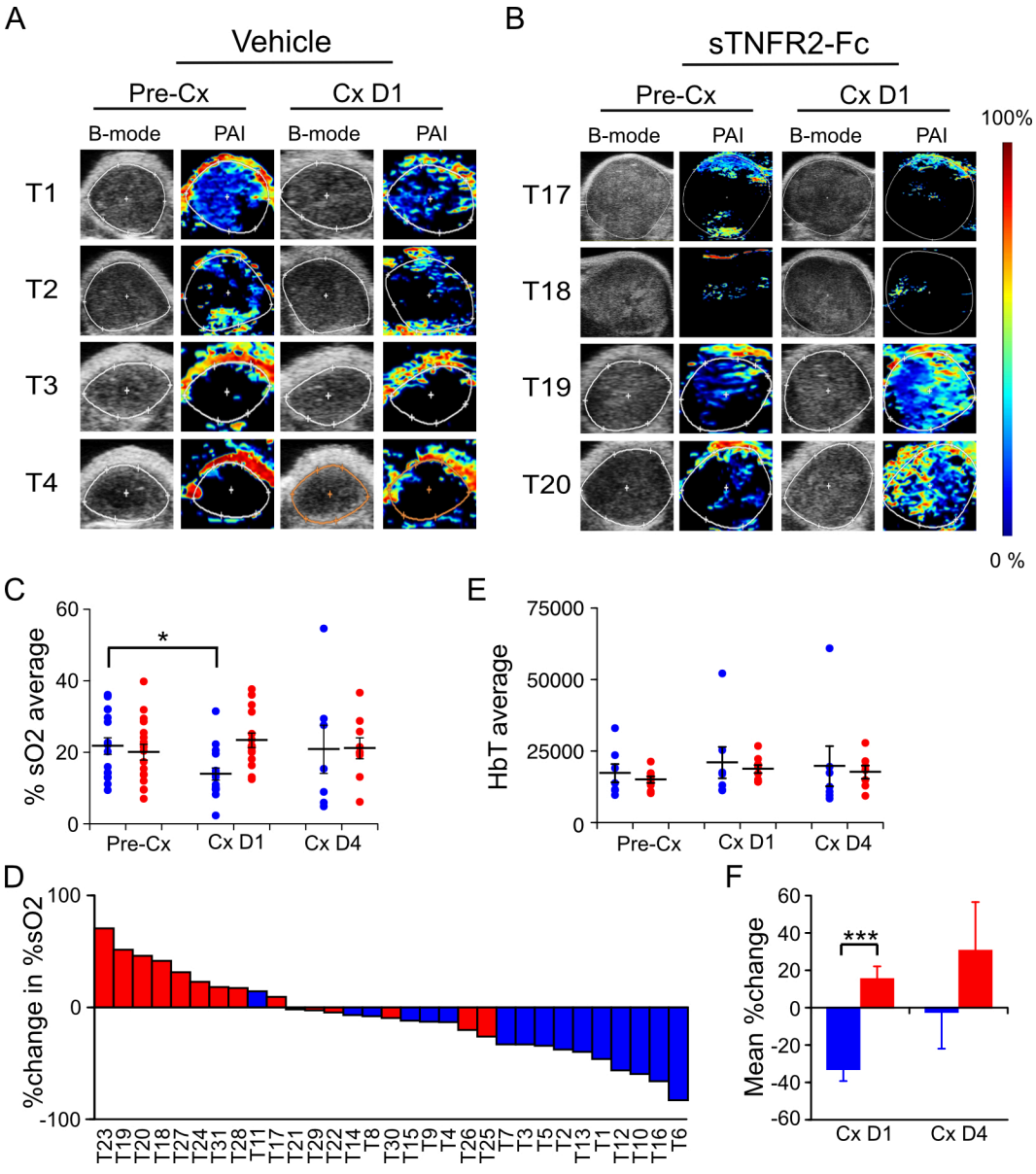

Legend for Figure 4. Castration induced hypoxia in Myc-CaP tumor was reversed by TNF blockade. **A** and **B,** Photoacoustic images (PAI, pseudo-colored) and ultrasound (B-mode) of Myc-CaP subcutaneous tumor of four tumors from each group, pre and post castration from vehicle treated mice

(**A**), or sTNFR2-Fc treated mice (**B**). **C**, Mean PAI signal (%sO_2) from tumors pre-castration (n=16), and at one (n=15), and at four (n=9) days post-castration in vehicle treated (blue) or in sTNFR2-Fc treated (red) mice. **D,** Mean total hemoglobin from tumors pre-castration (n=16), and at one (n=16), and at four (n=14) days post-castration in vehicle treated (blue) or in sTNFR2-Fc treated (red) mice. **E,** Waterfall plot of change in %sO_2 in individual tumors at one day post-castration versus pre-Cx. **F,** Mean change in paired measures of %sO_2 pre-castration versus D1 or D4 post-castration. Mean (columns) and SEM (bars). *$p<0.05$, ***$p<0.001$.

Accomplished under Aim 2

Major Task 2 remains to be done. We will use samples from Aim 3 for this, which we plan to begin as soon as possible.

Accomplished under Aim 3

In Aim 3, we continue to collect and store samples for future batch-wise analysis. A large batch was sent to the Genomics core this month and we will begin analyzing the data soon.

What opportunities for training and professional development has the project provided?
Nothing to report.

How were the results disseminated to communities of interest?
Nothing to report.

What do you plan to do during the next reporting period to accomplish the goals?

As noted above we will complete the remainder of Aims 2 and 3. And begin preparing the publications.

4. IMPACT:

What was the impact on the development of the principal disciplines of the project?

We demonstrated that TNF signaling is required for both the regression and recurrence phases of the response to castration. We also demonstrating that CCL2 signaling is required for the recurrence phase only – it has no role in regression. Moreover, blockade of late TNF signaling phenocopies the blockade of CCL2 signaling, consistent with a molecular mechanism in which TNF acts via NFkB to promote CCL2 expression (a well-described gene regulatory event). We have previously demonstrated that following the initial regression response to castration there is an increase in the stem-like cell character of the tumor cells which likely contributes to high NFkB levels.

What was the impact on other disciplines?
Nothing to report

What was the impact on technology transfer?
Nothing to report

What was the impact on society beyond science and technology?
Nothing to report

5. CHANGES/PROBLEMS:

Changes in approach and reasons for change

Nothing to report

Changes that had a significant impact on expenditures

Nothing to report

Significant changes in use or care of human subjects, vertebrate animals, biohazards, and/or select agents

Significant changes in use or care of human subjects

Nothing to report

Significant changes in use or care of vertebrate animals

Nothing to report

Significant changes in use of biohazards and/or select agents

Nothing to report

6. PRODUCTS:

Publications.

Nothing to report

Other publications, conference papers and presentations.

Nothing to report

Website(s) or other Internet site(s)

Nothing to report

Technologies or techniques

Nothing to report

Inventions, patent applications, and/or licenses

Nothing to report

Other Products

Nothing to report

7. PARTICIPANTS & OTHER COLLABORATING ORGANIZATIONS

What individuals worked on the project?

John Krolewski, MD PhD. PI. 2.4 Calendar Months.

- Dr. Krolewski lead the project and analysis of the data for manuscript #2.

Kent Nastiuk, PhD. HRI Scientist (promoted to Assistant Member and changed role to co-I), 3.6 Calendar Months

- Dr. Nastiuk helped to supervise the post-doctoral fellow in the lab, managed the imaging experiments and assisted with the analysis of the data. He is leading the writing for manuscript #1.

Kevin Eng, PhD. Biostatistician, 0.96 Calendar Months

- Dr. Eng assisted with statistical analysis of the regression and recurrence kinetics.

Aerken Maolake, PhD. Post-doc. 6 Calendar Months.

- Dr. Maolake carried out the bench work on the project.

Gurkamal Chatta, MD. Co-investigator. 0.24 Calendar Months

- Dr. Chatta assisted with Aim 3.

Bo Xu, MD, PhD. Co-investigator. 0.24 Calendar Months

- Dr. Xu assisted with Aim 3.

Has there been a change in the active other support of the PD/PI(s) or senior/key personnel since the last reporting period?

Nothing to Report

What other organizations were involved as partners?

None

8. SPECIAL REPORTING REQUIREMENTS

Nothing to report

9. APPENDICES:

Nothing to report